JOURNAL OF GEOPHYSICAL RESEARCH, VOL. 91, NO. D10, PAGES 10,818–10,824, SEPTEMBER 20, 1986

Recombination of Atomic Oxygen Near the Mesopause: Interpretation of Rocket Data

G. BRASSEUR[1]

Institut d'Aéronomie Spatiale, Brussels, Belgium

D. OFFERMANN

University of Wuppertal, Federal Republic of Germany

From the observations of atomic oxygen concentrations during the Energy Budget Campaign 1980, heating rates in the lower thermosphere at high latitude for late fall are derived and are found to be rather high. Useful information is also inferred for the vertical transport of mass and heat at these heights. The eddy diffusion coefficient which is derived from the data decreases with decreasing altitude below 100 km and reaches a minimum value of the order of 10 $m^2 s^{-1}$ near the mesopause. Such low value implies a low minimum concentration of nitric oxide (10^5–10^6 cm^{-3}) near 80 km.

1. INTRODUCTION

Recombination of atomic oxygen is one of the most important heating mechanisms in the lower thermosphere and is an important step in the conversion of solar radiative energy into atmospheric thermal energy. Indeed, the solar ultraviolet radiation is absorbed by molecular oxygen (O_2) which is photodissociated to produce two oxygen atoms (O):

$$O_2 + h\nu \xrightarrow{J_{O_2}} O + O \quad (1)$$

On the average, the thermospheric production of odd oxygen which produces a downward flux of atomic oxygen must be balanced by a destruction occurring at lower levels. This simple one-dimensional picture, however, applies to globally mean steady state conditions, but in the real world, the flux divergence results not only from vertical transport but also from horizontal (meridional and zonal) mass exchanges.

The lifetime of atomic oxygen above the mesopause is large (5 days at 90 km, 1 month at 95 km, 2 months at 100 km [see *Brasseur and Solomon*, 1984]), so that these atoms can be transported (together with their related enthalpy) to relatively long distances ($\sim$5000 km at 95 km, assuming a meridional velocity of 2 m s^{-1}) before they recombine. Thus the average meridional flow which is directed from the summer to the winter hemisphere transports atomic oxygen from a region where it is produced by solar light to a region where it is destroyed by recombination. In this latter part of the atmosphere, the net vertical mass flow is a strong subsidence which transports species such as O, NO or CO downward. Turbulent diffusion resulting, for instance, essentially from the breaking of gravity waves acts as a significant transport mechanism responsible for strong mixing and dissipation above the stratopause.

The one-dimensional approach which is used in the following discussion is thus only a first approximation but should give a rough picture for the overall vertical transport and its variability during winter days at high latitudes.

[1]Now at National Center for Atmospheric Research, Boulder, Colorado.

Paper number 6D0244.
0148-0227/86/006D-0244$05.00

Vertical profiles of atomic oxygen density were measured at several occasions during the Energy Budget Campaign 1980 [*Dickinson et al.*, 1985]. A very preliminary analysis of these data with respect to heating rates and vertical eddy transport was performed by *Offermann* [1985]. The purpose of the present paper is to present a more detailed analysis of these high-latitude data and to derive quantitative values of the heating rates in the 80- to 100-km range. Furthermore, assuming that the measured profiles represent typical conditions, an order of magnitude of the eddy diffusion coefficient K can be derived in the lower thermosphere by inverting the continuity/transport equation of odd oxygen.

2. THE DATA

The atomic oxygen abundance in the thermosphere was obtained from rocket-borne UV resonance lamps launched together with many other rockets from Esrange, Sweden (67.9° N, 21.1°E), on November 10, 1980, at 2345 LT (salvo C) and on December 1, 1980, at 0012 LT (salvo A2), respectively [*Dickinson et al.*, 1985]. During salvo C the geomagnetic conditions were completely quiet, while during salvo A2 they were strongly disturbed (for details, see *Offermann* [1985]). Figure 1 shows the two atomic profiles as they are used for the purpose of the present study. In order to deal with vertical distributions which are representative of average conditions over a sufficiently long period of time, small structures and waves, which are transient phenomena, have been removed from the observed profiles.

The two profiles are significantly different, as the first, which was measured during quiet conditions, peaks with a concentration of 1.1×10^{12} cm^{-3} at 96 km, while the second, measured during strong geomagnetic disturbance, reaches a maximum of 4.5×10^{11} cm^{-3} at 94 km. It appears difficult to relate the differences in atomic oxygen profiles to the differences in magnetic activity. It is rather believed that they are due to differences in the dynamical state of the atmosphere at lower altitudes (for details, see *Offermann* [1985]).

Comparison of the smoothed curves with other measurements of atomic oxygen shows that the salvo C profile is approximately representative of normal atmospheric conditions, as far as profile shape and absolute number density are concerned. The profile of salvo A2, on the contrary, appears to be an example for an atmosphere with strong dynam-

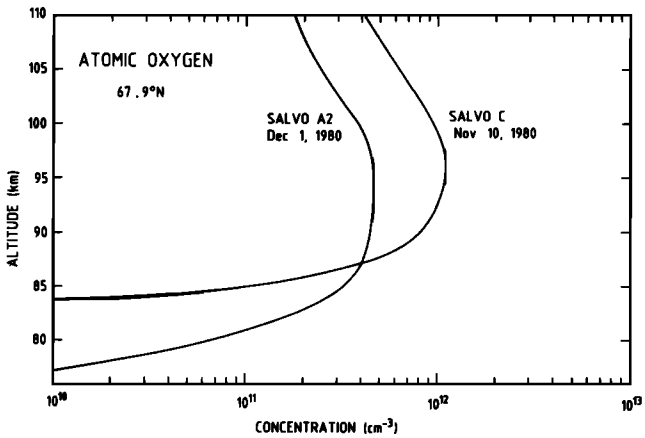

Fig. 1. Vertical distribution of the atomic oxygen concentration observed at 67.9°N latitude on November 10, 1980, and December 1, 1980. The curves have been slightly smoothed to remove the small-scale structure.

ical or turbulent disturbance present [*Offermann et al.*, 1981; *Kopp et al.*, 1985; P. H. G. Dickinson, private communication, 1985].

The distributions of temperature and concentrations of O, O_2, and N_2 adopted for the present calculations are given in Tables 1 and 2. Temperatures were derived by downward integration of total atmospheric densities. Density profiles were measured during the salvoes by active and passive falling spheres [*Philbrick et al.*, 1985; *Schmidlin et al.*, 1985]. Several temperature profiles obtained on one day were averaged and smoothed to eliminate small-scale structures [*Kuechler*, 1985]. For November 10–11, 1980, the temperature above 90 km was taken from the U.S. Standard Atmosphere (1976) with a smooth transition to the falling sphere data. Mass spectrometer data confirm that this is a reasonable approximation to the mean temperature profile on this particular day [*Dickinson et al.*, 1985].

Number densities of N_2 and O_2 in Table 1 were obtained from the smoothed mass density profiles by assuming a N_2/O_2 density ratio as given in the U.S. Standard Atmosphere (1976). On November 10–11, 1980, no falling sphere data were available above 90 km. There was, however, a mass spectrometer measurement of the N_2 number density above 98 km. This was used instead, and the gap between the two data sets was bridged by interpolation.

TABLE 1. Vertical Distribution of the Temperature and the Concentration of O, O_2, and N_2 Adopted in the Case of Salvo C (November 10–11, 1980)

Altitude, km	Temperature, K	Concentration: Atomic Oxygen, cm^{-3}	Molecular Oxygen, cm^{-3}	Molecular Nitrogen, cm^{-3}
84	203.8	1.85 (10)	3.07 (13)	1.14 (14)
86	201.6	2.15 (11)	2.37	8.84 (13)
88	196.5	5.20	1.85	6.91
90	192.2	8.12	1.38 (13)	5.18
92	191.2	9.78 (11)	9.90 (12)	3.75
94	189.7	1.07 (12)	6.38	2.46
96	189.8	1.09	3.99	1.57
98	192.2	1.05 (12)	2.52	1.03 (13)
100	195.6	9.44 (11)	1.61	6.89 (12)
102	199.9	8.14	1.03 (12)	4.69
104	205.7	6.88	6.70 (11)	3.27
106	213.1	5.84	4.33	2.29
108	223.7	4.96	2.82	1.62
110	240.8	4.22	1.75	1.10 (12)
112	264.0	3.62	1.16 (11)	7.85 (11)
114	288.0	3.14	7.90 (10)	5.76
116	315.3	2.76	5.51	4.27
118	339.3	2.46	3.95	3.21
120	359.0	2.26 (11)	2.89 (10)	2.45 (11)

Read 1.85 (10) as 1.85×10^{10}.

TABLE 2. Vertical Distribution of the Temperature and the Concentration of O, O_2, and N_2 Adopted in the case of Salvo A2 (December 1, 1980)

Altitude, km	Temperature, K	Concentration: Atomic Oxygen, cm^{-3}	Molecular Oxygen, cm^{-3}	Molecular Nitrogen, cm^{-3}
78	223.9	2.0 (10)	7.15 (13)	2.67 (14)
80	221.8	6.7	5.26	1.96
82	221.5	1.47 (11)	3.63	1.36 (14)
84	220.6	2.66	2.64	9.82 (13)
86	218.2	3.74	1.97	7.36
88	213.5	4.19	1.53	5.73
90	206.9	4.42	1.14 (13)	4.27
92	202.6	4.53	8.65 (12)	3.27
94	195.9	4.56	6.39	2.46
96	191.8	4.49	4.53	1.79
98	185.9	4.31	3.22	1.32 (13)
100	185.4	3.85	2.16	9.26 (12)
102	189.1	3.12	1.45 (12)	6.59
104	201.4	2.61	9.24 (11)	4.52
105	226.7	2.23	5.66	2.99
108	254.6	1.96	3.32	1.91
110	284.7	1.77	1.89	1.19 (12)
112	318.7	1.61	1.18 (11)	8.02 (11)
114	352.8	1.46	7.69 (10)	5.60
116	386.9	1.34	5.45	4.22
118	417.5	1.22 (11)	4.07 (10)	3.31 (11)

3. The Chemical Scheme

In the region near 100-km altitude, the behavior of O and O_2 can be described to a good approximation by a "pure oxygen" chemistry. In this case, in addition to the photodissociation of O_2, one has to consider the recombination of atomic oxygen by the following processes:

$$O + O + M \xrightarrow{k_1} O_2 + M \quad (+\varepsilon_1) \tag{2}$$

$$O + O_2 + M \xrightarrow{k_2} O_3 + M \quad (+\varepsilon_2) \tag{3}$$

$$O + O_3 \xrightarrow{k_3} 2O_2 \quad (+\varepsilon_3) \tag{4}$$

where M (mainly O_2 or N_2) is an atmospheric molecule acting as third body in (2) and (3). The rate constants can be expressed as

$$k_1 = 4.7 \times 10^{-33} (300/T)^2 \quad cm^6\ s^{-1}$$

$$k_2 = 6.2 \times 10^{-34} (300/T)^2 \quad cm^6\ s^{-1}$$

$$k_3 = 1.5 \times 10^{-11} \exp(-2218/T) \quad cm^3\ s^{-1}$$

The release of energy by these chemical processes is given by (see, for example, *Brasseur and Solomon* [1984]) $\varepsilon_1 = 5.12$ eV, $\varepsilon_2 = 1.05$ eV, and $\varepsilon_3 = 4.06$ eV.

Below 90 km the influence of the fast reacting hydrogen species becomes significant for odd oxygen destruction, so that the following additional reactions have to be considered:

$$H + O_3 \xrightarrow{k_4} OH + O_2 \quad (+\varepsilon_4) \tag{5}$$

$$OH + O \xrightarrow{k_5} H + O_2 \quad (+\varepsilon_5) \tag{6}$$

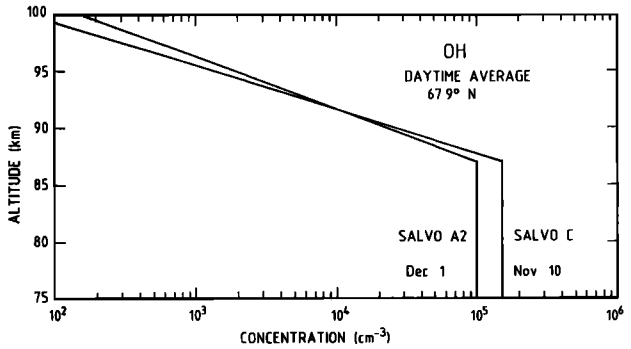

Fig. 2. Daytime average of the OH concentration versus altitude. Working values adopted for the present calculations are in good agreement with the figures provided by a full diurnal model at 67.9°N on November 10 and December 1.

$$HO_2 + O \xrightarrow{k_6} OH + O_2 \qquad (+\varepsilon_6) \tag{7}$$

$$H + O_2 + M \xrightarrow{k_7} HO_2 + M \qquad (+\varepsilon_7) \tag{8}$$

with

$$k_4 = 1.4 \times 10^{-10} \exp(-470/T) \quad cm^3\ s^{-1}$$

$$k_5 = 2.2 \times 10^{11} \exp(117/T) \quad cm^3\ s^{-1}$$

$$k_6 = 3.0 \times 10^{11} \exp(200/T) \quad cm^3\ s^{-1}$$

$$k_7 = 5.5 \times 10^{-32} (300/T)^{1.6} \quad cm^6\ s^{-1}$$

The corresponding energy releases for these reactions are $\varepsilon_4 = 3.34$ eV, $\varepsilon_5 = 0.72$ eV, $\varepsilon_6 = 2.39$ eV, and $\varepsilon_7 = 2.0$ eV. These numbers can be approximately converted to kcal/mol by multiplying them by 23.

The energy released by reactions (2) to (8) is given by

$$E = \varepsilon_1 k_1[M][O]^2 + \varepsilon_2 k_2[M][O_2][O] + \varepsilon_3 k_3[O_3][O] + \varepsilon_4 k_4[H][O_3] + \varepsilon_5 k_5[OH][O] + \varepsilon_6 k_6 + [HO_2][O] + \varepsilon_7 k_7[M][H][O_2] \tag{9}$$

When adopting photochemical equilibrium conditions for OH and HO_2 (neglecting the external sources and sinks for total odd hydrogen),

$$k_5[O][OH] = k_6[O][HO_2] + k_4[H][O_3] \tag{10}$$

$$k_7[M][H][O_2] = k_6[O][HO_2] \tag{11}$$

together with the energy conservation relations

$$\varepsilon_1 = \varepsilon_5 + \varepsilon_6 + \varepsilon_7$$

$$\varepsilon_3 = \varepsilon_4 + \varepsilon_5$$

one obtains the simplified relation for the energy release

$$E = \varepsilon_1 k_1[M][O]^2 + \varepsilon_2 k_2[M][O_2][O] + \varepsilon_3 k_3[O_3][O] + \varepsilon_{eff} k_5[OH][O] \tag{12}$$

where

$$\varepsilon_{eff} = \frac{\varepsilon_1 k_7[M][O_2] + \varepsilon_3 k_4[O_3]}{k_7[M][O_2] + k_4[O_3]} \tag{13}$$

Since $\varepsilon_1 = 5.11$ eV and $\varepsilon_3 = 4.06$ eV, an intermediate value of $\varepsilon_{eff} = 4.5$ eV can be adopted without appreciable error. The calculation of E requires, beside the specified values of [O], $[O_2]$, [M], and T given in Tables 1 and 2, the concentration of ozone and of the hydroxyl radical. For the first of these components it is assumed that O_3 is photochemically controlled by O [*Brasseur and Solomon*, 1984]. The calculation of the OH concentration is not straightforward, since it depends on the water vapor abundance, which is dependent on dynamical and photochemical conditions and is thus highly variable in space and time. Figure 2 shows the profiles of the diurnally averaged OH concentration adopted in the present study for the November 10 and December 1 experiments. These high-latitude winter values are very close to the figures obtained from a full diurnal model in which the water vapor mixing ratio is 4.2 parts per million by volume (ppmv) at 85 km, 2.2 ppmv at 90 km, and 1.3 ppmv at 95 km. In order to obtain the 24-hour average of the OH concentration, the values quoted in Figure 2 were multiplied by $T_d/24$, where T_d is the length of the day which is equal to 9.6 hours in the case of salvo C and 8.2 hours for salvo A2. Because of the high variability of the water vapor amount (e.g., a factor of 10), one should expect significant variations in the hydroxyl radical concentrations. This uncertainty introduces probably the largest error in the present calculation, and the profiles displayed in Figure 2 should thus be considered as a working model. On the other hand, it must be noted that the water vapor mixing ratios assumed above are presumably on the low side. This is shown by *Grossmann et al.* [1985], who obtained considerably higher values from two far infrared measurements at this time of the year. (One of these measurements was taken during the Energy Budget Campaign.) The OH values adopted here should therefore be on the low side, and the derived profiles of transport coefficients may be considered as upper limits.

As it is assumed that the oxygen distributions are typical of quiet and active dynamical states of the atmosphere, the one-dimensional steady state continuity equation for odd oxygen O_x (essentially atomic oxygen at these heights) can be used to infer the transport parameters in the lower thermosphere. If $\Phi(O_x)$ is the vertical flux of O_x, this equation is

$$\frac{d\Phi(O_x)}{dz} + 2k_1[M][O]^2 + 2k_3[O][O_3] + k_4[O_3][H] + k_5[O][OH] + k_6[O][HO_2] = 2J_{O_2}[O_2] \tag{14}$$

or, neglecting (4) and making use of the balance equation for OH,

$$\frac{d\Phi(O_x)}{dz} + 2k_1[M][O]^2 + 2k_5[OH][O] = 2J_{O_2}[O_2] \tag{15}$$

As the mass of atomic oxygen is significantly smaller than the average molecular mass of air in the lower thermosphere, the transport of O_x needs to be represented in terms of both eddy diffusion and molecular diffusion. The mean vertical flux of O_x in the range 80–100 km can thus be expressed as

$$\Phi(O_x) = -K[M] \frac{\partial}{\partial z}\left(\frac{[O]}{[M]}\right) - D\left\{\frac{\partial[O]}{\partial z} + \frac{[O]}{H_1} + \frac{[O]}{T}\frac{\partial T}{\partial z}\right\} \tag{16}$$

where $D = 1 \times 10^{17} T^{0.75}/[M]$ cm^2 s^{-1} [*Banks and Kockarts*, 1973] is the molecular diffusion coefficient for atomic oxygen in air, T is the temperature, and H_1 is the scale height of atomic oxygen. The flux due to molecular diffusion is species-dependent (through the value of D and H_1), while the eddy diffusion flux is generally assumed to be species-independent. It has been shown, however [*Strobel*, 1981; *Schoeberl et al.*, 1983; *Garcia and Solomon*, 1985; *Strobel et al.*, 1985], that as species may be transported by chemical eddies related, for example, to gravity wave breaking, the strength of their vertical eddy diffusion coefficient depends on their chemical life-

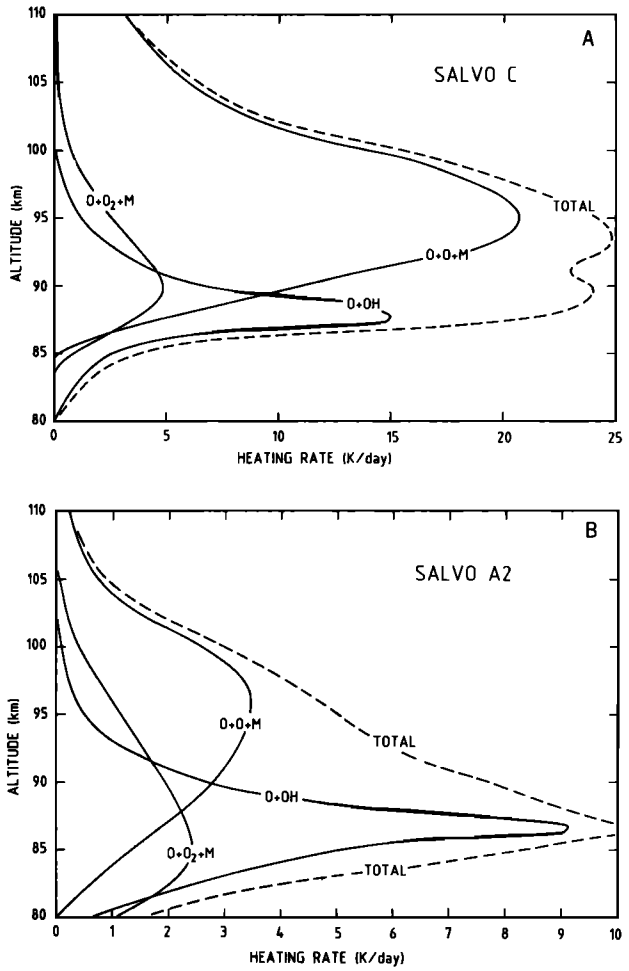

Fig. 3. Heating rate (in kelvins per day) resulting from the recombination of atomic oxygen during (*a*) salvo C and (*b*) salvo A2 of the Energy Budget Campaign.

time. The value of the K coefficient derived from the vertical distribution of a given chemical constituent (for example, atomic oxygen) is thus not strictly applicable to other constituents. This point was also made for long-lived species in the stratosphere (J. R. Holton, private communication, 1985), where transport is related to planetary wave activity. In essentially all one-dimensional model calculations, however, identical eddy diffusion coefficients are used for all species. The derivation through (15) and (16) of an exchange coefficient K is thus useful for practical model studies, as this coefficient accounts for all vertical exchange processes involved in the transport of odd oxygen (beside molecular diffusion), including gravity wave breaking.

4. Calculated Heating Rates and Eddy Diffusion Coefficients

4.1. *Heating Rates*

The vertical distribution of the 24-hour averaged heating rate due to the energy release by the several chemical reactions is displayed in Figure 3*a* and 3*b* for the two measurement days. It can be seen that in both cases the recombination of atomic oxygen by (2) is the largest heat source, leading for example to a heating rate of close to 20 K/day at 95 km in the case of salvo C. Reaction (3) plays a role which becomes comparable to that of reaction (2) only below 87–90 km. The contribution of (4) is negligible. Near the mesopause the reactions involving hydrogen radicals play a significant role in the thermal budget. The resulting heating rate in the two cases is different by more than a factor of 2. Its implication for the heat budget in the lower thermosphere will be discussed in section 5.

4.2. *Eddy Diffusion Coefficients*

Direct and indirect estimates of turbulence parameters in the 80- to 120-km range have been discussed recently by *Danilov* [1984]. In this study the vertical transport is calculated by integrating downward equation (15), starting at 120 km, where a boundary condition is specified. If one assumes that at this level, the entire vertical flux Φ can be expressed in terms of pure molecular diffusion, one obtains at 120 km, with the temperature and atomic oxygen concentration as given in Table 1, $\Phi = -1.7 \times 10^{12}$ cm^{-2} s^{-1} for salvo C and -0.84×10^{12} cm^{-2} s^{-1} for salvo A2. The vertical downward flux obtained by integration of (15) is shown between 85- and 100-km altitude in Figure 4. It can be seen that the conditions associated with the two rocket flights were significantly different. The flux from the thermosphere appears to be quite larger in the case of salvo C, but it decreases more rapidly with decreasing altitude than does that of salvo A2 owing to a smaller vertical exchange rate and a larger recombination.

Figure 5 shows the vertical distribution of the K coefficient obtained by inverting (16), after removing the contribution of molecular diffusion to the downward flux. The uncertainty represented in the figure by shaded regions corresponds to a variation of 10% in the specified atomic oxygen flux at 120 km. Moreover, the calculated upper limit is obtained by reducing the OH concentration by a factor of 3 in order to account for a possible overestimation in the water vapor content. This reduction is probably larger than the real uncertainty, so that the calculated upper limit corresponds to a maximum maximorum of the eddy diffusion coefficient near the mesopause.

For both salvoes the magnitude of the eddy diffusion coefficient is estimated to be of the order of 100 to 200 m^2 s^{-1} at 100-km altitude. Below this level the K coefficient decreases with a gradient which is considerably weaker for salvo A2 than for salvo C. At 90 km, for example, the value of K is reduced to about 15 m^2 s^{-1} in the first case but is still close to 90 m^2 s^{-1} in the second case.

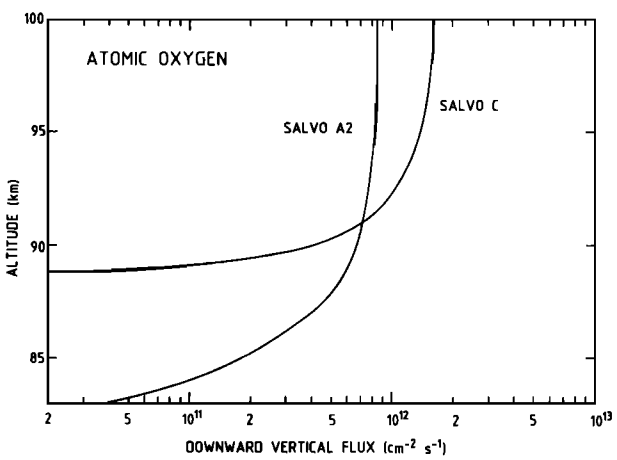

Fig. 4. Downward flux of atomic oxygen calculated by integrating the continuity equation of odd oxygen and using the atomic oxygen data obtained during salvoes C and A2.

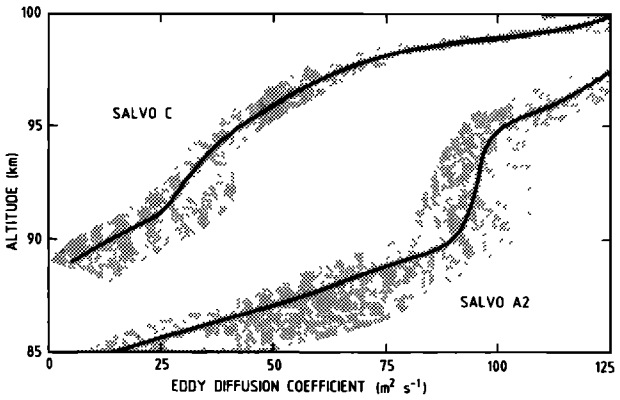

Fig. 5. Vertical distribution of the eddy diffusion coefficient inferred from the profile of the atomic oxygen concentration as shown in Figure 1. The uncertainty represented by shaded areas corresponds to a variation of 10% in the atomic oxygen flux specified at 120 km as the boundary condition and to the effect of a reduction by a factor of 3 of the OH concentration.

5. Discussion

The eddy diffusion coefficients obtained from these purely chemical considerations based on the behavior of atomic oxygen are shown in Figure 6 together with the profiles derived at lower altitude during the same campaign by *Thrane et al.* [1985]. The latter values were obtained using electrostatic ion probes mounted on the front part of several rocket payloads. Although the two studies use completely different physical concepts to define the eddy diffusion coefficient, they seem to come in agreement near the mesopause level, especially if one considers the two curves obtained from the same salvo (C). At this level the K coefficient is characterized by a minimum of the order of 10 m^2 s^{-1}. The existence of this minimum, which is consistent with the theory of gravity wave breaking by *Lindzen* [1981], was already mentioned by *Thrane et al.* [1985] and was also found more recently by *Blix et al.* [1985] during the Middle Atmosphere Program (MAP)/Winter in Northern Europe (WINE) Campaign. Indeed, the data obtained during this campaign by electrostatic ion-probes on seven rockets launched from Andøya, Norway (winter 1983–1984), show in certain cases very rapid increases in the eddy coefficient values just above the mesopause, in good agreement with our profiles derived from the atomic oxygen measurements. In all cases the K value between 80 and 90 km is significantly smaller than the value adopted in most one-dimensional models and is indeed a factor of 10 lower than the value suggested in the U.S. Standard Atmosphere (1976) or derived, as an upper limit, by *Johnson and Wilkins* [1965*a*, *b*] to account for the vertical heat transport between 50 and 110 km. The K profile obtained for the most representative case (salvo C) is, however, in good agreement with the low values derived between 95 and 100 km in winter by *Alcayde et al.* [1979] from temperature measurements inferred in the lower thermosphere from incoherent scatter data. Figure 7 shows two profiles of the eddy diffusion profile obtained during the MAP/WINE campaign together with our values and with the profile derived by *Allen et al.* [1981].

In order to estimate the effect of this small eddy diffusion coefficient on some trace species that are sensitive to transport processes, such as nitric oxide, the vertical distribution of the NO concentration has been calculated by means of a one-dimensional model [*Brasseur et al.*, 1982] using the two different profiles of K shown in Figure 8*a*. The high value ($K \simeq 200$ m^2 s^{-1} between 80 and 100 km) leads to a strong downward flux of NO and a concentration that is never significantly lower than 10^7 cm^{-3} if the upper boundary condition at 100 km is chosen to be 10^8 cm^{-3} (see Figure 8*b*). The K profile labeled "low," which is characterized by a deep minimum at 85 km in accord with our analysis based on atomic oxygen data (essentially salvo C), leads to significantly lower nitric oxide concentrations, in much better agreement with observations (see, for example, *Tohmatsu and Iwagami* [1976] and *Baker et al.* [1977]). The altitude of the concentration minimum is also 5 km higher than that in the previous case. It should be noted that as the value of the K coefficient is dependent on the lifetime of the species which is transported, the eddy diffusion coefficient required to explain the vertical profile of NO might be significantly different from the profile derived from atomic oxygen observations. *Strobel et al.* [1985] have noted that K(NO) should be smaller than K(O) in the mesosphere but larger than K(O) above 90-km altitude.

The heating rates obtained from the atomic oxygen recombination are significantly different on the two occasions considered. However, they have in common that they are large in comparison with other energetic processes involved in the heat budget of the lower thermosphere. Competing processes such as particle precipitation, infrared emission, and wave dissipation were also measured during the Energy Budget Campaign and analyzed at 90-km altitude by *Offermann* [1985]. There appears to be a considerable problem of energy balance which becomes particularly serious if one uses the eddy diffusion coefficients derived in the previous section to calculate the energy transport. Indeed, the minima in the eddy profiles around the mesopause, shown in Figures 5 to 7, are deep enough to prevent virtually all the energy from being transported to lower altitudes. The steep gradients in the K profile above the mesopause imply a turbulent heating at this level rather than a cooling as is usually assumed. In other words, the effect of gravity wave breaking obviously does not help in bringing the atmosphere closer to energy balance. The long-standing problem of energy imbalance at the mesopause is thus obviously revived under high-latitude winter conditions. It should be noted that the problem becomes even worse if adiabatic heating by subsidence is included.

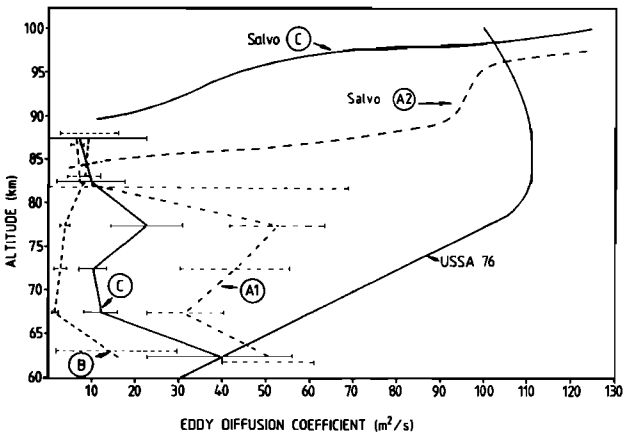

Fig. 6. Eddy diffusion coefficients derived from the atomic oxygen densities measured during salvoes C and A2 (higher altitudes) and from ion fluctuations observed during salvoes C and A1 of the same campaign (lower altitudes). The profile of the eddy diffusion coefficient recommended in the U.S. Standard Atmosphere (1976) is also indicated.

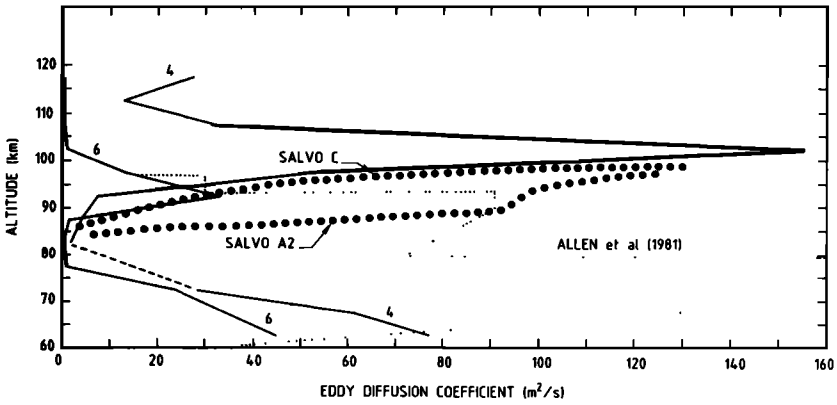

Fig. 7. Comparison between the eddy diffusion coefficients inferred from the atomic oxygen densities measured during the Energy Budget Campaign (salvoes C and A2) with similar profiles derived from measurements of ion fluctuation profiles obtained during the MAP/WINE campaign [*Blix et al.*, 1985]. The profile suggested by *Allen et al.* [1981] is also indicated.

6. Conclusions

Measurements of the atomic oxygen concentration in the lower thermosphere reported during the Energy Budget Campaign have been used to derive thermodynamic and dynamic parameters in the altitude range of about 85 to 100 km. The two profiles measured during salvo C and salvo A2 are believed to be representative of normal and dynamically disturbed conditions, respectively. Both calculated heating rates and eddy diffusion coefficients are significantly different in the two cases. For example, a large (factor of 5) difference in the contribution to the heating rate of the O + O + M reaction is observed. In both cases, however, the odd hydrogen chemistry contributes significantly to the heating rate in a narrow altitude range just above the mesopause.

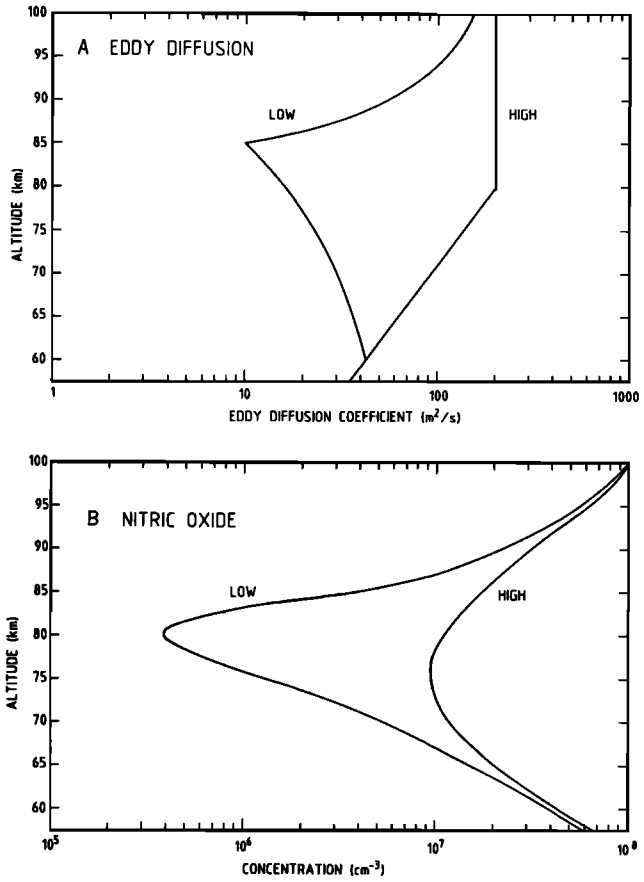

Fig. 8. Vertical profiles of the eddy diffusion coefficients (Figure 8*a*) adopted to calculate the two vertical distributions of the nitric oxide concentration (Figure 8*b*). The curves labeled "low" correspond to an eddy diffusion profile similar to the values corresponding to salvo C, while the curves labeled "high" refer to values of the eddy diffusion coefficient as used in some current one-dimensional models (200 $m^2 s^{-1}$ in the lower thermosphere).

Considerable differences are also observed in the strength of the net vertical transport. However, these differences are not large enough to fill the minimum derived for the eddy diffusion coefficient near 85 km. This minimum is also present in the K profiles derived by *Thrane et al.* [1985] and *Blix et al.* [1985], even during very turbulent periods. The thermosphere is thus only weakly dynamically coupled with the lower atmospheric layers, although in certain conditions and at selected locations, a downward transport of species such as nitric oxide or carbon monoxide should be possible and in the case of NO is even observed [*Russell et al.*, 1984], in good agreement with theoretical analysis [*Frederick and Orsini*, 1982; *Solomon et al.*, 1982; *Brasseur*, 1982]. Absolute magnitudes of heating rates indicate strong energy budget imbalances on both occasions analyzed. It appears that a strong cooling mechanism is required that has yet to be determined. Further analyses of the physical mechanisms responsible for heat and mass exchanges in the lower thermosphere are required as concerns seasonal and latitudinal variations as well as occurrence frequency.

References

Alcayde, D., J. Fontanari, G. Kockarts, P. Bauer, and R. Bernard, Temperature, molecular nitrogen concentration and turbulence in the lower thermosphere inferred from incoherent scatter data, *Ann. Geophys.*, *35*, 41–51, 1979.

Allen, M., Y. L. Yung, and J. W. Waters, Vertical transport and photochemistry in the terrestrial mesosphere and lower thermosphere (50–120 km), *J. Geophys. Res.*, *86*, 3617–3627, 1981.

Baker, K. D., A. F. Nagy, R. O. Olsen, E. S. Oran, J. Randhawa, D. F. Strobel, and T. Tohmatsu, Measurement of the nitric oxide altitude distribution in the mid-latitude mesosphere, *J. Geophys. Res.*, *82*, 3281–3296, 1977.

Banks, P. M., and G. Kockarts, *Aeronomy*, part B, 355 pp., Academic, Orlando, Fla., 1973.

Blix, T. A., E. V. Thrane, and O. Andreassen, Middle atmosphere turbulence as determined by ion-probes, *Eur. Space Agency Spec. Publ.*, *229*, 371–375, 1985.

Brasseur, G., *Physique et chimie de l'atmosphère moyenne*, 310 pp., Masson, Paris, 1982.

Brasseur, G., and S. Solomon, *Aeronomy of the Middle Atmosphere: Chemistry and Physics of the Stratosphere and Mesosphere*, 441 pp., D. Reidel, Hingham, Mass., 1984.

Brasseur, G., A. Roucour, and A. de Rudder, The natural and perturbed ozonosphere, in *Proceedings of the International Conference on Environmental Pollution*, edited by A. Anagnostopoulos, pp. 839–910, University of Thessaloniki, Thessaloniki, Greece, 1982.

Danilov, A. D., Direct and indirect estimates of turbulence around the turbopause, *Adv. Space Res.*, *4*, 67–78, 1984.

Dickinson, P. H. G., U. von Zahn, K. D. Baker, and D. B. Jenkins, Lower thermosphere densities of N_2, O and Ar under high latitude winter conditions, *J. Atmos. Terr. Phys.*, *47*, 283–290, 1985.

Frederick, J. E., and N. Orsini, The distribution and variability of mesospheric odd nitrogen: A theoretical investigation, *J. Atmos. Terr. Phys.*, *44*, 479–488, 1982.

Garcia, R. R., and S. Solomon, The effect of breaking gravity waves on the dynamics and chemical composition of the mesosphere and lower thermosphere, *J. Geophys. Res.*, *90*, 3850–3868, 1985.

Grossmann, K. U., W. G. Frings, D. Offermann, L. Andre, E. Kopp, and D. Krankowsky, Concentrations of H_2O and NO in the mesosphere and the lower thermosphere at high latitudes, *J. Atmos. Terr. Phys.*, *47*, 291–300, 1985.

Johnson, F. S., and B. Gottlieb, Eddy mixing and circulation at ionospheric levels, *Planet. Space Sci.*, *18*, 1707–1718, 1970.

Johnson, F. S., and E. M. Wilkins, Thermal upper limit on eddy diffusion in the mesosphere and lower thermosphere, *J. Geophys. Res.*, *70*, 1281–1284, 1965*a*.

Johnson, F. S., and E. M. Wilkins, Correction to "Thermal upper limit on eddy diffusion in the mesosphere and lower thermosphere", *J. Geophys. Res.*, *70*, 4063, 1965*b*.

Kopp, E., F. Bertin, L. G. Bjorn, P. H. G. Dickinson, C. R. Philbrick, and G. Witt, The 'CAMP' campaign 1982, *Eur. Space Agency Spec. Publ.*, *229*, 117–123, 1985.

Kuechler, R., Analyse von Temperature-und Windmessungen mit Raketèn während der Energie-Bilanzkampagne, 1980, technical report, Phys. Dep., Univ. of Wuppertal, Federal Republic of Germany, 1985.

Lindzen, R. S., Turbulence and stress owing to gravity wave and tidal breakdown, *J. Geophys. Res.*, *86*, 9707–9714, 1981.

Offermann, D., The Energy Budget Campaign 1980: Introductory review, *J. Atmos. Terr. Phys.*, *47*, 1–26, 1985.

Offermann, D., V. Friedrich, P. Ross, and U. von Zahn, Neutral gas composition measurements between 80 and 120 km, *Planet. Space Sci.*, *29*, 747–764, 1981.

Philbrick, C. R., F. J. Schmidlin, K. U. Grossman, G. Lange, D. Offermann, K. D. Baker, D. Krankowsky, and U. von Zahn, Density and temperature structure over northern Europe, *J. Atmos. Terr. Phys.*, *47*, 159–172, 1985.

Russell, J. M., III, S. Solomon, L. L. Gordley, E. E. Remsberg, and L. B. Callis, The variability of stratospheric and mesospheric NO_2 in the polar winter night observed by LIMS, *J. Geophys. Res.*, *89*, 7267–7275, 1984.

Schmidlin, F. J., M. Carlson, D. Rees, D. Offermann, C. R. Philbrick, and H. U. Widdel, Wind structure and variability in the middle atmosphere during the November 1980 Energy Budget Campaign, *J. Atmos. Terr. Phys.*, *47*, 183–193, 1985.

Schoeberl, M. R., D. F. Strobel, and J. A. Apruzese, A numerical model of gravity wave breaking and stress in the mesosphere, *J. Geophys. Res.*, *88*, 5249–5259, 1983.

Solomon, S., P. J. Crutzen, and R. G. Roble, Photochemical coupling between the thermosphere and the lower atmosphere, 1, Odd nitrogen from 50 to 120 km, *J. Geophys. Res.*, *87*, 7206–7220, 1982.

Strob !, D. F., Parameterization of linear wave chemical transport in planetary atmospheres by eddy diffusion, *J. Geophys. Res.*, *86*, 9806–9810, 1981.

Strobel, D. F., J. P. Apruzese, and M. R. Schoeberl, Energy balance constraints on gravity wave–induced eddy diffusion in the mesosphere and lower thermosphere, *J. Geophys. Res.*, *90*, 13,067–13,072, 1985.

Thrane, E. V., Ø. Andreassen, T. Blix, B. Grandal, A. Brekke, C. R. Philbrick, F. J. Schmidlin, H. U. Widdel, U. von Zahn, and F. J. Lubken, Neutral air turbulence in the upper atmosphere observed during the Energy Budget Campaign, *J. Atmos. Terr. Phys.*, *47*, 243–264, 1985.

Tohmatsu, T., and N. Iwagami, Measurement of nitric oxide abundance in the equatorial upper atmosphere, *J. Geomagn. Geoelectr.*, *28*, 343–358, 1976.

G. Brasseur, National Center for Atmospheric Research, P.O. Box 3000, Boulder, CO 80307.

D. Offermann, University of Wuppertal, D-5600 Wuppertal 1, Federal Republic of Germany.

(Received January 2, 1986;
revised April 22, 1986;
accepted April 24, 1986.)